



GHGT-12

Water Solubility in CO₂ Mixtures: Experimental and Modelling Investigation

Mohammad Ahmad^{a*} and Sander Gersen^a

^aDNV-GL Oil & Gas, Energieweg 17, 9743 AN Groningen, The Netherlands

Abstract

The capture of CO₂ from power plants and other large industrial sources is offering a main solution to reduce CO₂ emissions. The captured mixture will contain impurities like nitrogen, argon, oxygen, water and some toxic elements like sulfur and nitrogen oxides, the types and quantities of which depend on the type of fuel and the capture process. The presence of free water formation in the transportation pipeline causes severe corrosion problems, flow assurance failure and might damage valves and instrumentations. In the presence of free water, CO₂ dissolves in the aqueous phase and will partly ionize to form a weak acid. Thus, free water formation should be avoided.

This work aims to investigate the solubility of water in CO₂ mixtures under pipeline operation conditions in the temperature range of (5 – 35 °C) and the pressure range of (90 – 150 bar). A test set up was constructed, which consists of a high pressure reactor in which a CO₂ mixture containing water at initial soluble conditions was prepared. The purpose of this study is to identify the maximum water content level which could be allowed in CO₂ transportation pipelines. The experimental data generated were then compared to the calculations of two mixture models: the GERG-2008 model and the EOS-CG model.

© 2014 The Authors. Published by Elsevier Ltd. This is an open access article under the CC BY-NC-ND license (<http://creativecommons.org/licenses/by-nc-nd/3.0/>).

Peer-review under responsibility of the Organizing Committee of GHGT-12

Keywords: Carbon capture and storage, pipelines, water solubility, equation of states.

1. Introduction

The capture of CO₂ from large fossil fuel, biomass energy facilities and from other large CO₂ point sources has become relevant within the concept to mitigate CO₂ emissions via Carbon Capture and Storage. A big part of this captured CO₂ stream will be transported at high pressure dense phase conditions and stored in offshore underground depleted oil and gas fields. CO₂ is also transported in offshore pipelines to be used for enhanced oil and gas recovery. The capture process may result in impurities like nitrogen, argon, oxygen, methane, water and some toxic elements like sulfur and nitrogen oxides. The types and amount of impurities depend on the type of fuel, the type of the capture process and any gas treatment steps either prior or subsequent to the CO₂ capture [1].

* Corresponding author. Tel.: +31.6.15094945; fax: +31.50.7009858.

E-mail address: mohammad.ahmad@dnvgl.com

Having impurities in the CO₂ steam will cause expansion of the liquid-vapour phase envelope and will increase or drop the dew-point and the bubble point pressures ([2], [3] and [4]). The increase of the bubble point pressure would mean that pipeline operators have to transport dense or liquid CO₂ at higher pressures to avoid phase change in their pipelines. The presence of free water formations has an even more severe impact mainly because of the corrosion issue. CO₂ will then dissolve in the aqueous phase and partly ionize to form a weak acid. When partly hydrated, CO₂ will slowly dissolve in water and form carbonic acid. Thus, to keep low corrosion rates, the CO₂ should be dry or the water should be fully dissolved at all operation conditions. With free water formation present in the pipeline, the corrosion rates could be in the order of mm every year [5]. The water solubility, on the other hand, depends on the type and the amount of impurities present in the CO₂ stream and on the pipeline operation conditions of pressure and temperature [6] and [7]. 500 ppm is typical accepted water content by CO₂ pipeline operators, considered to be with a good safety margin for avoiding corrosion ([8] and [9]). The first experimental work carried out by Ahmad et al. [10] has shown for the different examined CO₂ mixtures that water fractions of 500 ppm were fully soluble at pressures down to 90 bar and at temperatures down to 5 °C. However, other experts ask for full dehydration for avoiding corrosion risks by achieving a water content of 50 ppm, or a concentration of no more than 60% of the dew point at worst case conditions [11].

To set the water content specifications, the designers and the operators of the CO₂ pipeline transmission systems should have data on the solubility of water in CO₂ mixtures, and the models describing the solubility should be verified and validated. There is a limited amount of experimental data available in the literature on the solubility of water in CO₂. In this study, the solubility of water in CO₂ mixtures was studied. An experimental set up was constructed with a high pressure reactor in which well-defined CO₂ mixtures could be prepared and where pressure and temperature could be controlled and varied. A silicon chip based hygrometer sensor was connected to the reactor to measure water content. The sensor showed very rapid response, high accuracy to humidity changes and insensitivity to sample flow rate. Because of the water high polarity and water stickiness issues, a special attention was given to the set up material in particular the sealing, fittings, tubing and to the sampling process. The experimental data generated were compared to two mixture models explicit in the Helmholtz free energy. The first model is the GERG-2008 [12] that was developed for natural gas mixtures and is capable to describe the CO₂ mixtures studied in this work as well. The second is the EOS-CG model [13] that is based on the same mathematical structure as the GERG-2008, with special focus on CO₂ mixtures and humid gases.

2. Experimental Test Set Up

The experimental test set up is made up of a high pressure reactor in which gases can be injected and mixtures can be prepared. The pressure and temperature inside the reactor is flexibly controlled. The reactor has a total volume of 15 ml. It consists of a cylindrical sapphire tube (Fig. 1) that is closed by two lids and covered by a double jacket of polycarbonate. The temperature of the mixture inside the reactor is controlled using water filled refrigerated and a heating circulator connected to the double jacket, allowing the temperature inside the reactor to be varied from 4 to 40 °C. The reactor pressure could be changed using a piston system installed inside the sapphire to provide the volume variation capability. The capstan was placed vertically so that a magnetic rod (stirrer) could be installed at the bottom lid of the reactor for gas mixing purposes.

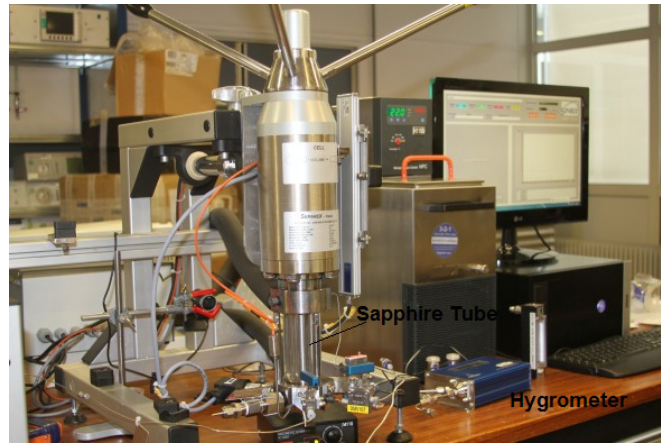


Fig. 1. Photo of the experimental system.

The CO₂ is injected into the reactor using a pump with a head pressure of 200 bar. Gas mixtures of well known composition are supplied to the reactor from high pressure calibrated bottles. Water is introduced inside the reactor using small syringes at atmospheric pressure (1 bar) where water is injected into a heated line and is then flushed into the reactor. The reactor internal walls are well treated to eliminate any water stickiness problems. Fig. 2 shows a schematic representation of the reactor. The pressure was measured using precise pressure transmitters at two locations, at the syringe pump side and inside the reactor side at the gage block location. The gage block contains a safety valve that opens if over pressurization inside the system occurs. The capillary connection lines have very small volumes compared to that of the reactor and the syringe pump. A set of standard high pressure valves, rated 1000 bar, was used allowing a certain connection and isolation flexibility of the reactor, the syringe pump and the supply source.

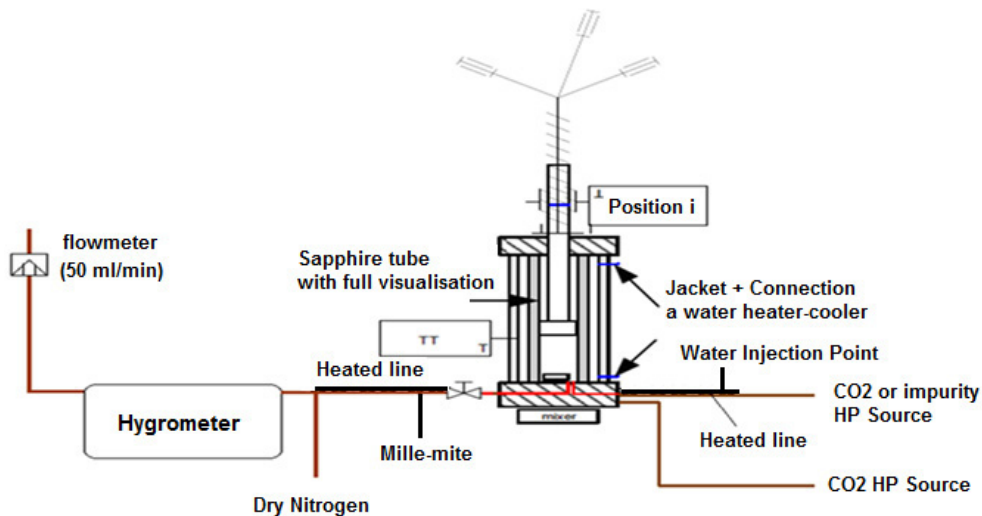


Fig. 2. Schematic representation of the experimental set up.

The water content was measured from samples taken from the reactor through a heated line using a silicon chip hygrometer. During the sampling process, a volume flow rate of 50ml/min of vapour supply was needed to get a representative water content value. The sensor acts as a capacitor which interacts at the dielectric level with the hydrogen bonding of water to cause a dielectric change. After reading the water content of a certain sample, the sensor is self-heated to get rid of any absorbed moisture. The sensor responds to water vapour pressure in equilibrium. Thus, in order to dry it further, flushing using dry nitrogen was required after each sampling process.

3. Experimental Procedure

The first experimental step was to insure the elimination of any water residuals in the reactor or in the connection lines prior to the experiment, so the system was first filled with pure CO₂, heated and flushed for a couple of times. Afterwards, the mixtures of water, impurities and CO₂ in fully soluble conditions are then prepared inside the reactor. First, the water is injected inside the heated (up to 80 °C) supply line of the reactor using a hand syringe. Next, the water was flushed into the reactor using either pure CO₂ supply stream (experiments with pure CO₂-water mixtures) from the pump, or impurity supply stream (experiments with CO₂-impurity-water) from high pressure bottles.

Knowing the initial experiment conditions of pressure and temperature and the targeted mixture composition (pure CO₂ or CO₂-impurity mixture) enables us to deduce the amount of water to be injected and the injection pressure value of the impurity. After injecting water, the impurity and finally the CO₂, the mixture in the reactor could be then left to homogenize using the stirrer for a couple of hours at high temperature (40 °C) conditions that provide high water solubility conditions. At the end of experiment preparation phase, the mixtures prepared inside the reactor will have the required water mass content (in soluble conditions) in a mixture composition at a certain pressure conditions and a temperature of 40 °C. For verification purposes, the reading of the hygrometer for the first sample taken from the reactor should indicate the exact water mass content of the mixture. A sample taken from the reactor undergoing gas chromatographic analysis (GC) will indicate the exact mixture composition. The uncertainty in the mixtures composition measurements using the GC is 0.01%. The uncertainty in the temperature measurement inside the cell is 0.5 °C and that of the pressure is 0.3%.

After the preparation of the mixture, the sampling process starts. In every sample, 0.1 to 0.2 g of CO₂ is taken out from the reactor with a flow rate of 50ml/min for a couple of minutes. The water content of the sample is measured using the hygrometer and compared to the first reading. During the sampling process, the pressure in the reactor is kept constant by dropping the piston level of 1-3 % of the cell height, whereas the temperature is dropped (using the water heat exchanger) after each sample, until the hygrometer reads lower reading. The drop in the water mass content in the sample read by the hygrometer is explained by the formation of free water on the reactor wall, indicating that water dew-point temperature has been reached. The uncertainty in the detection of the dew-point is 1.2 °C.

4. Models Used

The two models used for comparison with the experimental data, GERG-2008 and EOS-CG models, are based on the same multi-fluid approach with different adjusted mixture parameters. Both models are explicit in the reduced Helmholtz free energy $\alpha = a(\rho, T, \bar{x})/RT$, which is a function of density ρ , temperature T , and mixture composition (or mole fraction) \bar{x} (R is the gas constant). The reduced Helmholtz free energy can be expressed by an ideal-gas part α^o and a residual contribution α^r according to

$$\alpha(\delta, \tau, \bar{x}) = \frac{a}{RT} = \alpha^o(\rho, T, \bar{x}) + \alpha^r(\delta, \tau, \bar{x}) \tag{1}$$

Where the reduced mixture density δ and the inverse reduced mixture temperature τ are given by

$$\delta = \rho/\rho_r(\bar{x}) \quad \text{and} \quad \tau = T_r(\bar{x})/T \tag{2}$$

The functional form of the reducing functions $\rho_r(\bar{x})$ and $T_r(\bar{x})$ is given by [12]:

$$\frac{1}{\rho_r(\bar{x})} = \sum_{i=1}^N x_i^2 \frac{1}{\rho_{c,i}} + \sum_{i=1}^{N-1} \sum_{j=i+1}^N 2x_i x_j \beta_{v,ij} \gamma_{v,ij} \frac{x_i + x_j}{\beta_{v,ij}^2 x_i + x_j} \frac{1}{8} \left(\frac{1}{\rho_{c,i}^{1/3}} + \frac{1}{\rho_{c,j}^{1/3}} \right)^3, \tag{3}$$

and

$$T_r(\bar{x}) = \sum_{i=1}^N x_i^2 T_{c,i} + \sum_{i=1}^{N-1} \sum_{j=i+1}^N 2x_i x_j \beta_{T,ij} \gamma_{T,ij} \frac{x_i + x_j}{\beta_{T,ij}^2 x_i + x_j} (T_{c,i} T_{c,j})^{0.5}, \tag{4}$$

$\beta_{v,ij}$, $\gamma_{v,ij}$, $\beta_{T,ij}$, and $\gamma_{T,ij}$ are adjustable binary reducing parameters, and ρ_c and T_c are the critical densities and temperatures of the mixture pure components.

Unlike the residual part α^r of the Helmholtz free energy model which is evaluated at reduced mixture parameters, using composition-dependent reducing functions $\rho_r(\bar{x})$ and $T_r(\bar{x})$, the ideal-gas part α^o is evaluated at the non-reduced density ρ and temperature T . It is given by:

$$\alpha^o(\rho, T, \bar{x}) = \sum_{i=1}^N x_i \left[\alpha_{o,i}^o(\delta_{o,i}, \tau_{o,i}) + \ln x_i \right], \quad (5)$$

$\alpha_{o,i}^o$ and x_i are the dimensionless ideal-gas part of the Helmholtz free energy and the mole fraction of component i in the mixture, and N is the number of components in the mixture. The sum $x_i \ln x_i$ accounts for the entropy of mixing in the ideal mixture. The ideal-gas parts of the Helmholtz free energies of each pure component are evaluated at their component specific reduced parameters $\delta_{o,i}$ and $\tau_{o,i}$, which are given as follows:

$$\delta_{o,i} = \rho / \rho_{c,i} \quad \text{and} \quad \tau_{o,i} = T_{c,i} / T. \quad (6)$$

The residual part of the Helmholtz free energy of the mixture is given by the following equation:

$$\alpha^r(\delta, \tau, \bar{x}) = \sum_{i=1}^N x_i \alpha_{o,i}^r(\delta, \tau) + \Delta \alpha^r(\delta, \tau, \bar{x}), \quad (7)$$

$\alpha_{o,i}^r$ is the residual part of the reduced Helmholtz free energy of component i and $\Delta \alpha^r$ is the so-called *departure function*, constituted by:

$$\Delta \alpha^r(\delta, \tau, \bar{x}) = \sum_{i=1}^{N-1} \sum_{j=i+1}^N x_i x_j F_{ij} \alpha_{ij}^r(\delta, \tau), \quad (8)$$

The binary departure function α_{ij}^r for the components i and j and the weighing factor F_{ij} are introduced by [10]. The mathematical structure of the binary departure function used in the GERG-2008 model is a combination of polynomial and exponential terms specifically developed for mixtures. It reads:

$$\begin{aligned} \alpha_{ij, \text{GERG-2008}}^r(\delta, \tau) = & \sum_{k=1}^{K_{\text{pol},ij}} n_{ij,k} \delta^{d_{ij,k}} \tau^{l_{ij,k}} \\ & + \sum_{k=K_{\text{pol},ij}+1}^{K_{\text{pol},ij}+K_{\text{spec},ij}} n_{ij,k} \delta^{d_{ij,k}} \tau^{l_{ij,k}} \exp \left[-\eta_{ij,k} (\delta - \varepsilon_{ij,k})^2 - \beta_{ij,k} (\delta - \gamma_{ij,k}) \right]. \end{aligned} \quad (9)$$

On the other hand, the departure function in the EOS-CG model uses a simple form of exponential terms also used in common Helmholtz models for pure fluids. It is given by:

$$\begin{aligned} \alpha_{ij, \text{EOS-CG}}^r(\delta, \tau) = & \sum_{k=1}^{K_{\text{pol},ij}} n_{ij,k} \delta^{d_{ij,k}} \tau^{l_{ij,k}} + \sum_{k=K_{\text{pol},ij}+1}^{K_{\text{pol},ij}+K_{\text{exp},ij}} n_{ij,k} \delta^{d_{ij,k}} \tau^{l_{ij,k}} \exp(-\delta^{l_{ij,k}}) \\ & + \sum_{k=K_{\text{pol},ij}+K_{\text{exp},ij}+1}^{K_{\text{pol},ij}+K_{\text{exp},ij}+K_{\text{spec},ij}} n_{ij,k} \delta^{d_{ij,k}} \tau^{l_{ij,k}} \exp \left[-\eta_{ij,k} (\delta - \varepsilon_{ij,k})^2 - \beta_{ij,k} (\delta - \gamma_{ij,k}) \right]. \end{aligned} \quad (10)$$

The mixture models given in equations (1) to (10) are thus a combination of pure fluid contributions, namely $\alpha_{o,i}^o$ and $\alpha_{o,i}^r$, and mixture contributions, namely the reducing functions $\rho_r(\bar{x})$ and $T_r(\bar{x})$, and the binary departure functions α_{ij}^r . For the description of the pure fluid contributions [12] developed new short Helmholtz equations of state specifically designed to work well with mixture models, while in the EOS-CG model the reference Helmholtz equations were used. The models are adjusted to experimental mixture data by fitting the binary reducing parameters $\beta_{v,ij}$, $\gamma_{v,ij}$, $\beta_{r,ij}$, $\gamma_{r,ij}$ and, if necessary, the adjustable parameters in the binary departure function α_{ij}^r . The experimental data used for the parameter fitting of the EOS-CG model include properties in the homogeneous gas and liquid phases (densities, speed of sound data, heat capacities or excess enthalpies) as well as phase equilibrium measurement data (phase compositions at given temperature and pressure) over a

wide range of temperature, pressure and composition. The parameters were fitted by minimizing the sum of squares of the deviations between experimental and calculated property values, using a non-linear optimization algorithm. This method enables fitting to all kinds of available experimental data simultaneously without any pre-correlations [13].

5. Experimental data

The experimental data of water solubility in CO₂-O₂ mixtures with 2.5% O₂ is given in Fig. 3 as a function of pressure and temperature. The figure shows an increase in water solubility with the increase of temperature in the range of pressure and temperature tested. Maintaining constant pressure conditions of 90 bar, the water solubility increases from 991 ppm at 20 °C, to close to 1422 ppm at 33 °C and up to 1927 ppm at 41 °C. At constant pressure of 150 bar, the water solubility increases from 967 ppm at 12 °C, to close to 1422 ppm at 33 °C and up to 1927 ppm at 41 °C. The water solubility is also affected by the variation in pressure. An increased pressure was observed to increase the water solubility. However, the influence of temperature seems to be more prominent. An increase in temperature of 1 °C would raise the water solubility by 50 ppm, while an increase in pressure of 1 bar would raise the solubility by only 3 or 4 ppm. The increase in the solubility driven by the increase in the temperature or pressure conditions has been observed for the different CO₂ mixtures examined in this study.

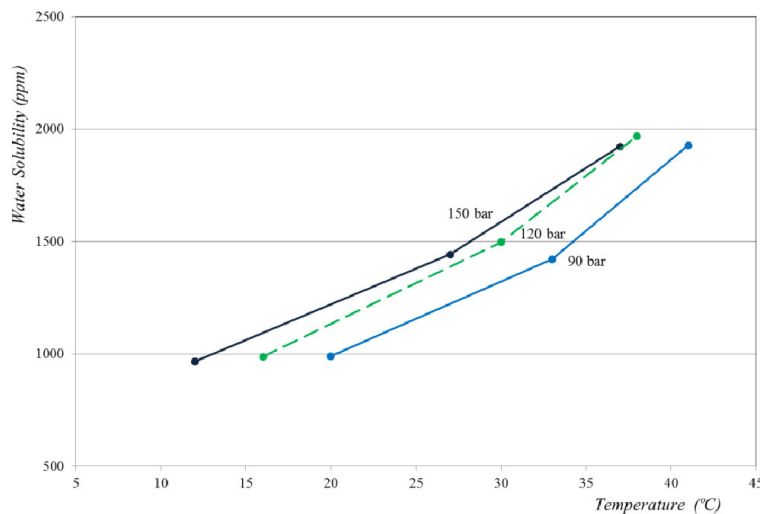


Fig. 3. Water solubility in CO₂-O₂ mixtures (2.5% O₂).

Fig. 4 shows the water solubility measurements for CO₂ mixtures with different impurities (2.5% of O₂, N₂ or CH₄) at constant pressure condition of 120 bar. A similar dependence of water solubility on temperature and pressure is observed with the different studied mixtures. The experimental data show a drop in the water solubility in the presence of impurities. Among the three examined mixtures with the three types of impurities, the data observed with both CO₂-N₂ and CO₂-O₂ mixtures were very similar with the lowest water solubility readings recorded for the CO₂-CH₄ mixtures. At a constant pressure of 120 bar, with pure CO₂ the water solubility increases from 1025 ppm at 15 °C, to 1460 ppm at 28 °C and up to 2100 ppm at 38 °C, while with CO₂-CH₄ mixtures (2.5% CH₄) the water solubility increases from 979 ppm at 17 °C, to 1496 ppm at 31 °C and up to 1968 ppm at 39 °C. The presence of 2.5% of any of N₂, O₂ or CH₄ in CO₂ lowers the water solubility limit by 75 ppm at minimum (low temperature) and 200 ppm at maximum (high temperature) depending on pressure and temperature.

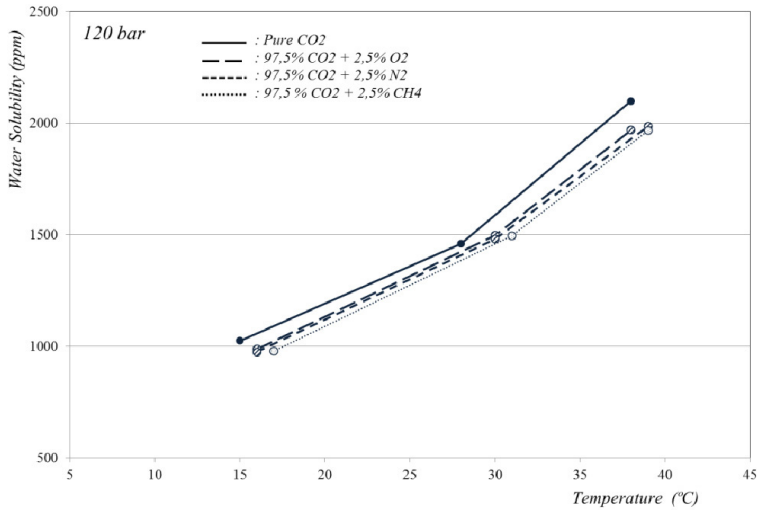


Fig. 4. Water solubility at 120 bar in pure CO₂ and in CO₂ with 2.5% of O₂, N₂ or CH₄.

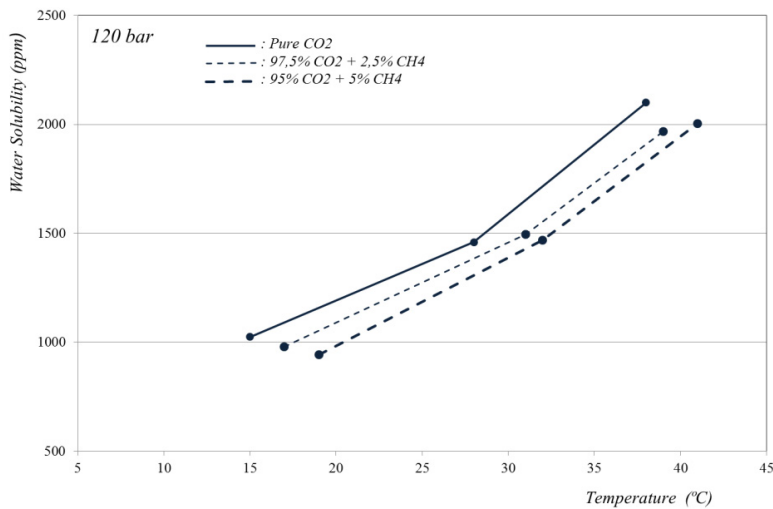


Fig. 5. Water solubility at 120 bar in CO₂ - CH₄ mixtures.

The effect of the amount of impurities on water solubility was also studied. Fig. 5 shows the water solubility data at 120 bar for a mixture of 2.5% methane and another with 5% methane in comparison with pure CO₂ data. The water solubility drops with the increase in the level of methane. The water solubility was 979 ppm at 17 °C with 2.5% methane, and 943 ppm at 19 °C with 5% methane. The solubility increases to 1496 ppm at 31 °C and then to 1968 ppm at 39 °C with 2.5% methane, while with 5% methane the solubility recorded was 1469 ppm at 32 °C and increased to 2005 ppm at 41 °C. The presence of 500 ppm of NO₂ or SO₂ in the CO₂ appears (Fig. 6) to have larger impact on water solubility in comparison with the other tested impurities. Fig. 6 shows a drop of water solubility of around 500 ppm at minimum (at low temperatures close to 15 °C) up to around 1000 ppm at maximum (at high temperatures close to 39 °C) upon the addition of 500 ppm of NO₂ in CO₂. A further drop of water solubility is observed with 500 ppm of SO₂.

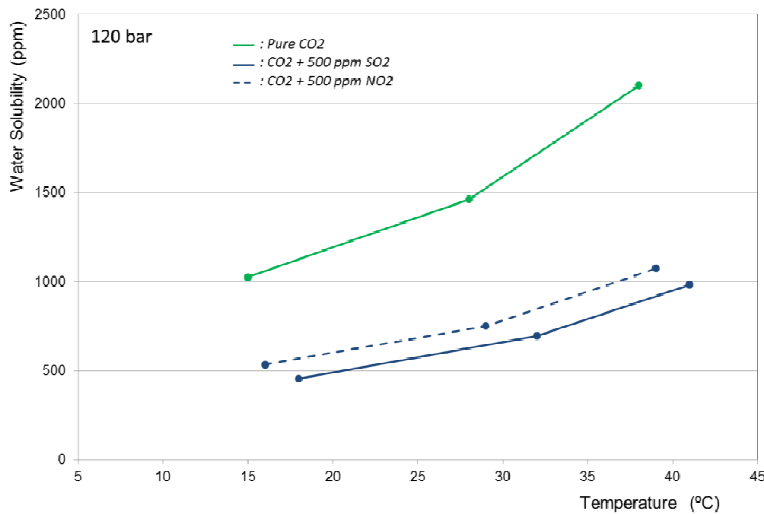


Fig. 6. Water solubility at 120 bar in CO₂ mixtures with SO₂ and NO₂.

The availability of water solubility data in pure CO₂ as well as in CO₂ with impurities is crucial to set up CO₂ mixtures specifications at the capture locations, and will have direct implication on the CO₂ pipeline design as well as on the pipeline operation envelope. In the different examined mixtures, a drop in the water solubility was observed at low pressures and temperatures or due to the presence of impurities. For setting up the allowable water level in CO₂ pipelines to avoid free water formation, the following considerations should be taken into account:

- The type and quantity of impurities downstream of the capture location which depend on the capture technique and the fuel type. It should be mentioned here that the CO₂ capture costs are greatly affected as CO₂ purity becomes more stringent.
- The influence the impurities first have on the liquid vapor phase transition zone of CO₂, and the fact that operational envelop should first be set to avoid any two phase flow in the pipeline.
- The influence that the impurities have on water solubility. In the presence of impurities either higher minimum pressures or temperatures should be maintained in the pipeline or further water drying should be carried out to avoid free water formations and corrosion problems.

Looking to the presented experimental data, 500 ppm of water were fully soluble at the conditions of minimum pressure (90 bar) and minimum temperature (5 °C) for the different tested mixtures except with the presence of NO₂ and SO₂. However, setting up allowable water content, attention should also be paid to the different pipeline operation regimes (system shut down, discharge or filling, and so on) and the risk of the consequent water formations because of the resulting low temperature and pressures.

6. Model calculations

The availability of experimental data is also crucial to assess and further develop physical models. The experimental results obtained at different pressures for water solubility in pure CO₂ (Fig. 7) and in CO₂-O₂ (figure 8) mixtures are compared to the predictions of the two models used in this study, the GERG-2008 and the EOS-CG. For both mixtures, the figures show a better performance of the GERG-2008 equation of state predicting water solubility in the range of pressure and temperature tested. The GERG-2008 calculations show a good agreement with the experimental data especially at high pressures (120 bar). At 90 bar (closer to the critical and phase transition zones), the model predictions slightly deteriorate for both pure CO₂ and CO₂-O₂ mixtures. The comparison with experimental data shows an average prediction error of around 200 ppm at 90 bar and less than 50 ppm at 120 bar. The model predicts the right dependency trend of water solubility as function of pressure and temperature.

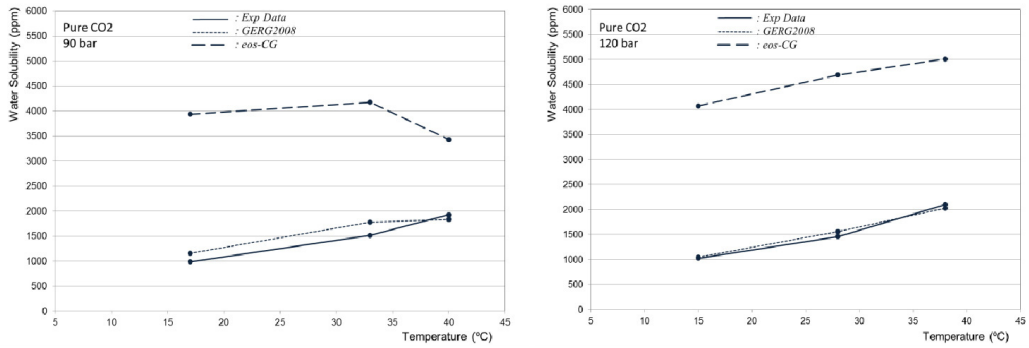


Fig. 7. Water solubility in pure CO₂ - Models prediction and experimental data. Solid Line: experimental data, long dashed line: EOS-CG, square dotted: GERG 2008.

The EOS-CG model shows the right trend predicting the water solubility with both pure CO₂ and CO₂-O₂ mixtures as function of temperature except at low pressure of 90 bar where an increase in temperature close to the critical zone results in a drop of water solubility. However and in comparison with the GERG-2008 model and for both presented mixtures, the EOS-CG model significantly overestimates the solubility of water for the different pressures and temperature examined, see Fig. 7 and 8. The comparison with experimental data shows an average prediction error reaching 400% with a remarkably better performance at 90 bar and at high temperatures. The quantitative agreement with the experimental can be further improved by fitting the interaction parameters to the obtained ternary high-pressure three-phase equilibrium data.

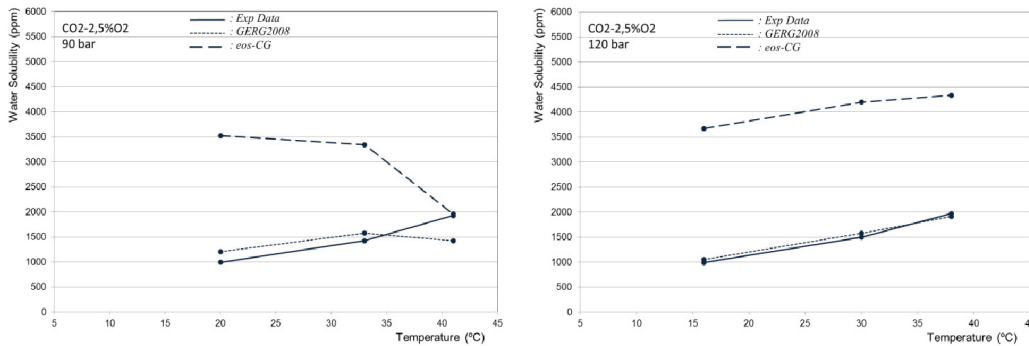


Fig. 8. Water solubility in pure CO₂-O₂ mixtures - Models prediction and experimental data. Solid Line: experimental data, long dashed line: EOS-CG, square dotted: GERG 2008.

7. Conclusions

Water solubility in CO₂ mixtures at pipeline operation conditions has been studied. An experimental set up was used to measure water solubility in pure CO₂ as well as in CO₂ mixtures. The accuracy of two mixture models, the GERG-2008 model and the EOS-CG model, was assessed using the measurement data. The experimental data and the different models predictions have been analyzed and the following conclusions can be made:

- In range of pressure and temperature studied and for the different tested mixtures, the water solubility increased with the increase in the temperature or pressure.
- For all studied ternary mixtures with 2.5% of a certain impurity, 500 ppm of water were fully soluble at the conditions of minimum pressure (90 bar) and minimum temperature (5 °C). However, with the presence of only 500 ppm of NO₂ or SO₂, and in comparison with the other mixtures, the water solubility has drastically dropped to the borders of 500 ppm.

- The experimental data showed a drop in the water solubility limit of 75 ppm and down to 200 ppm with the presence of 2.5 % of any of N₂, O₂ or CH₄ in CO₂. The water solubility in CO₂ was lowered by around 500/700 ppm at minimum and around 1000/1200 ppm at maximum upon the addition of 500 ppm of NO₂/SO₂ respectively.
- The GERG-2008 equation of state showed better predictions of water solubility in comparison with the EOS-CG model for the tested mixtures and in the range of pressure and temperature studied. The calculations could be however, improved by fitting the interaction parameters to the obtained ternary high-pressure three-phase equilibrium data.

Acknowledgement

This research has been financed by a grant from the Energy Delta Gas Research (EDGaR) program. EDGaR is co-financed by the Northern Netherlands Provinces, the European Fund for Regional Development, the Ministry of Economic Affairs, Agriculture and Innovation and the Province of Groningen. We also gratefully acknowledge the financial support from the N.V. Nederlandse Gasunie.

References

- [1] Van Dijk, H. Edgar CO₂ purity: types and quantities of impurities related to CO₂ point source and capture technology. ECN report: ECN-E-12-054, 2012.
- [2] Chapoy A, Burgass R, Tohidi B, Austell J M, Eickhoff C. . Effect of Common Impurities on the Phase Behavior of Carbon-Dioxide-Rich Systems: Minimizing the Risk of Hydrate Formation and Two-Phase Flow. SPE Journal. Volume 16, Number 4, 2011.
- [3] Goos E, Riedel U, Zhao L, Blum L. Phase diagrams of CO₂ and CO₂- N₂ gas mixtures and their application in compression processes. Energy Procedia 4, 3778-3785, 10th International Conference on Greenhouse Gas Control Technologies, 2011.
- [4] Ahmad, M Gernert, J, and Wilbers, E. Effect of impurities in captured CO₂ on liquid–vapor equilibrium. Fluid Phase Equilibria 363, 149– 155, 2014.
- [5] Seiersten M, Material selection for separation, transportation and disposal of CO₂, Proceedings Corrosion, National Association of Corrosion Engineers, paper 01042, 2001.
- [6] Austegard A and Barrio M. Project Internal Memo DYNAMIS: Inert components, solubility of water in CO₂ and mixtures of CO₂ and CO₂ hydrates, 2006.
- [7] Austegard A, Solbraa E, de Koeijer G and Mølnevik MJ. Thermodynamic Models for Calculating Mutual Solubilities in H₂O-CO₂-CH₄ mixtures. Chemical Engineering Research and Design (ChERD), Part A, 2005. Special issue: Carbon Capture and Storage, V 84, A9, pp. 781-794, 2006.
- [8] De Visser E, Hendriks C, Barrio M, Mølnevik M, de Koeijer G, Liljemark S, Le Gallo Y . Dynamis CO₂ quality recommendations”, International Journal of Greenhouse Gas Control 2, 478 – 484, 2008.
- [9] Mohitpour M, Golshan H, Murray A. *Pipeline Design & Construction*, A practical approach, The American Society of Mechanical Engineers, Three Park Avenue, New York, United States, 2003.
- [10] Ahmad A, Gersen S and Wilbers E. Solubility of water in CO₂ at pipeline operation conditions. International Journal of Chemical, Nuclear, Metallurgical and Materials Engineering 8, 4, 2014
- [11] Odru P, Broutin P, Fradet A, Saisset S, Ruer J, Girod L (2006) Technical and economic assessment of CO₂ transportation, IFP , GHGT-8, Trondheim, 2006.
- [12] Kunz, O and Wagner, W. The GERG-2008 Wide-Range Equation of State for Natural Gases and Other Mixtures: An Expansion of GERG-2004. Journal Chem. Eng. Data 57, 3032–3091, 2012.
- [13] Gernert, J. A New Helmholtz Energy Model for Humid Gases and CCS mixtures, Dissertation, Ruhr-Universität Bochum, 2013.